Intact hemisphere and corpus callosum compensate for visuomotor functions after early visual cortex damage

Alessia Celeghin[a,b], Matteo Diano[a,b], Beatrice de Gelder[c], Lawrence Weiskrantz[d,1], Carlo A. Marzi[e,f], and Marco Tamietto[a,b,d,1]

[a]Department of Psychology, University of Torino, 10123 Torino, Italy; [b]Department of Medical and Clinical Psychology, Tilburg University, 5000LE Tilburg, The Netherlands; [c]Department of Cognitive Neuroscience, Maastricht University, 6229ER Maastricht, The Netherlands; [d]Department of Experimental Psychology, University of Oxford, OX1 3UD Oxford, United Kingdom; [e]Department of Neuroscience, Biomedicine and Movement Sciences, University of Verona, 37134 Verona, Italy; and [f]National Institute of Neuroscience, 37134 Verona, Italy

Contributed by Lawrence Weiskrantz, October 12, 2017 (sent for review August 21, 2017; reviewed by Melvyn A. Goodale and Juha Silvanto)

Unilateral damage to the primary visual cortex (V1) leads to clinical blindness in the opposite visual hemifield, yet nonconscious ability to transform unseen visual input into motor output can be retained, a condition known as "blindsight." Here we combined psychophysics, functional magnetic resonance imaging, and tractography to investigate the functional and structural properties that enable the developing brain to partly overcome the effects of early V1 lesion in one blindsight patient. Visual stimuli appeared in either the intact or blind hemifield and simple responses were given with either the left or right hand, thereby creating conditions where visual input and motor output involve the same or opposite hemisphere. When the V1-damaged hemisphere was challenged by incoming visual stimuli, or controlled manual responses to these unseen stimuli, the corpus callosum (CC) dynamically recruited areas in the visual dorsal stream and premotor cortex of the intact hemisphere to compensate for altered visuomotor functions. These compensatory changes in functional brain activity were paralleled by increased connections in posterior regions of the CC, where fibers connecting homologous areas of the parietal cortex course.

blindsight | corpus callosum | plasticity | Poffenberger | tractography

Cortical damage results in overt sensory and cognitive deficits, yet functions may be partially retained and patients may recover some impaired abilities owing to neuronal reorganization (1). Compensation of cognitive and motor deficits after unilateral lesions to the frontal or parietal cortex has been extensively investigated in neurological patients (2, 3) as well as animal models (4), revealing transcallosal recruitment of homologous areas in the intact hemisphere. These findings outline the brain's degeneracy, a common property of biological systems that refers to the ability of structurally different elements to perform the same function or yield the same output (5). In contrast, the brain's ability to withstand visual loss following destruction of the primary visual cortex (V1) by takeover of the contralesional hemisphere is not yet understood.

A well-documented example of retained visuomotor capacities and functional recovery following V1 damage is "blindsight" (6, 7). In such a condition, visual stimuli presented in the clinically blind field can induce accurate motor responses, even though the sufferer denies conscious perception (8). Preserved visuomotor transformation in blindsight has been mainly related to the contribution of V1-independent pathways involving the visual dorsal stream (9, 10). In fact, surviving extrastriate areas in the hemisphere deprived of V1 can still receive visual input through ipsilateral projections from subcortical structures and then transfer sensory information to motor and premotor areas within the same hemisphere via association tracts (11). The present study tests the alternative, albeit not mutually exclusive, possibility that visual guidance of simple movements in the absence of V1 can be mediated by the functional compensation of the intact hemisphere through transcallosal interplay.

A simple unimanual response task to lateralized visual stimuli, known as the Poffenberger paradigm (12), has been traditionally used to sample interhemispheric transfer of basic visuomotor information (13) and can be usefully adapted to investigate the compensatory contribution of the intact hemisphere when V1 damage occurs. In the uncrossed hemifield/hand combinations [left visual field/left hand (LVF/LH) and right visual field/right hand (RVF/RH)] the hemisphere initially receiving the visual input is also controlling the motor output, whereas in the crossed combinations the hemisphere of stimulus entry is different from the one triggering motor response (LVF/RH and RVF/LH). To accomplish the task and translate the visual input into motor output, interhemispheric interaction is thus required only in the crossed combination. The time needed for interhemispheric transfer is reflected in slower reaction times (RTs) for the crossed vs. uncrossed conditions (4 ms on average), thus determining positive values when the crossed–uncrossed difference (CUD) is calculated (14). Concerning the neuronal underpinnings, there is convincing evidence that the corpus callosum (CC) is involved in exchanging visuomotor information across hemispheres, and the CUD is believed to reflect callosal conduction time (15). For example, patients with either surgical resection or genetic absence of the CC present a marked lengthening of the CUD (16). Moreover, evidence from fMRI studies in healthy participants has demonstrated selective activation of the CC in the crossed compared with the uncrossed conditions (17, 18).

Significance

The brain is resilient to injury and the possibility to promote recovery rests with our ability to understand the nature of postlesional plasticity. After damage to the visual cortex some patients with clinical blindness still react to unseen stimuli with appropriate motor responses, a phenomenon known as "blindsight." Our findings in one patient with early primary visual cortex damage suggest that this nonconscious visuomotor ability depends partly on the compensatory activity of the intact hemisphere, which can be dynamically recruited through the corpus callosum. Functional interactions between the damaged and intact hemisphere are subserved by changes in the underlying anatomical connections. These observations provide a framework for future investigations of functional recovery after brain damage and on mechanisms that mediate nonconscious abilities.

Author contributions: A.C., C.A.M., and M.T. designed research; B.d.G., C.A.M., and M.T. performed research; A.C., M.D., and M.T. analyzed data; A.C., L.W., and M.T. wrote the paper; and A.C., L.W., C.A.M., and M.T. interpreted data.

Reviewers: M.A.G., University of Western Ontario; and J.S., University of Westminster.

The authors declare no conflict of interest.

[1]To whom correspondence may be addressed. Email: larry.weiskrantz@psy.ox.ac.uk or marco.tamietto@unito.it.

This article contains supporting information online at www.pnas.org/lookup/suppl/doi:10.1073/pnas.1714801114/-/DCSupplemental.

Blindsight patient G.Y. is an ideal case study to examine whether the intact hemisphere can influence recovery of visuomotor functions after unilateral destruction of V1. First, his residual visual capacities have been repeatedly documented (19, 20), although not directly related to the compensatory role of the intact hemisphere during visuomotor integration. Second, his lesion has been functionally and anatomically verified to be complete (21) but confined to his left V1. Hence, extrastriate areas have remained intact and able to relay visual information either to anterior motor structures of the same hemisphere or to engage the opposite hemisphere through transcallosal projections. This offers the opportunity to tease apart intra- from interhemispheric mechanisms of adaptive changes in response to brain injury. Third, his lesion occurred at the age of 8 y (19), thereby exploiting the early brain's potential to recruit plasticity and compensate for altered visual experience during development. By testing patient G.Y. with the Poffenberger paradigm we took advantage of this interaction with unilateral hemispheric lesion, hemifield of visual stimulation, and unimanual response. In fact, randomly presenting visual stimuli either to the intact or damaged hemisphere during crossed or uncrossed response conditions allowed us to challenge the damaged hemisphere on a trial-by-trial basis and to study the translation of visual input into motor output within and between hemispheres. Moreover, in the context of this fully balanced, within-subject design, the patient served as his own control in a conservative approach.

Combining psychophysics, fMRI, and diffusion-weighted tractography we have been able to link behavioral alterations of visuomotor integration for unseen stimuli with the underlying functional and structural brain properties. As it happens, when visual stimuli were directed to the (left) damaged hemisphere, the CC dynamically recruited the (right) intact hemisphere even when interhemispheric coordination was not required in principle, as in the uncrossed condition. In this latter case, interhemispheric transfer occurred at the stages of sensory-motor integration (posterior parietal) as well as preparation of motor response (premotor) and involved enhanced activity in correspondingly different callosal sites. These compensatory changes in long-range communication between hemispheres were paralleled by microstructural modifications in the CC of G.Y. While the topographic and connectional organization of the CC in different subregions was comparable to that observed in age-matched controls, the density of transcallosal fiber tracts linking homologous regions of the posterior parietal cortex was significantly enhanced.

Results

Behavioral Results. The rationale of our analysis is straightforward (22). If visuomotor blindsight does not require the contribution of the intact hemisphere, then the same logic described above for neurotypical subjects applies. Hence, a positive CUD should be observed also when visual stimuli are presented to the blind hemifield because interhemispheric transfer is necessary only in the crossed visual field/response hand condition. Conversely, if nonconscious processing of visual information crucially engages the opposite intact hemisphere, then a negative CUD should obtain. This is so because a double interhemispheric transfer is needed when the unseen stimulus and the response hand are in the same side. The first passage enables visual input from ipsilesional and V1-independent pathways to reach the intact hemisphere, and a second transfer permits access back to motor centers controlling manual response in the visually damaged hemisphere (Fig. 1*A*).

Mean RTs were analyzed by a 2 × 2 repeated-measures ANOVA with visual field (LVF vs. RVF) and response (crossed vs. uncrossed) as within-subject factors. Neither main effect reached statistical significance, whereas the interaction did [F (1, 57) = 44.7, $P < 0.0001$] (Fig. 1*B*). During conscious perception, the crossed condition (LVF/RH) yielded significantly slower RTs than the uncrossed condition (LVF/LH), thus resulting in a positive CUD value (7.2 ms) ($P = 0.001$ by post hoc Bonferroni test). This value is approximately within the range of CUDs reported in previous experiments on healthy participants (23). The performance during nonconscious perception of stimuli in the RVF showed a strikingly opposite pattern and a negative CUD value (−9.9 ms), owing to faster RTs in the crossed (RVF/LH) than in the uncrossed condition (RVF/RH) ($P < 0.0001$).

Additionally, we estimated at each percentile the cumulative distribution functions (CDFs) of RTs in the four conditions separately. This chronometric description permits us to check whether the CUD differences observed on mean values occur throughout the whole distribution of RTs (Fig. 1*C*). When the stimuli were presented in the intact LVF, and thus consciously perceived, RTs in the crossed condition (LVF/RH) were significantly slower than those in the uncrossed condition (LVF/LH) throughout the entire CDFs, as assessed by Kolmogorov–Smirnov test ($P < 0.05$). The opposite pattern was observed during nonconscious presentation in the blind RVF, as the CDF for the crossed condition (RVF/LH) was significantly faster than for the uncrossed condition (RVF/RH) ($P < 0.005$).

fMRI Results. During conscious perception of LVF stimuli, the direct comparison between crossed and uncrossed responses revealed significant increase of bilateral brain activity in an extended network mainly involved in the visual guidance and preparation of motor responses (Fig. 2, *Upper* and Table S1). The crossed condition also enhanced fMRI response in the genu and rostral body of the CC, which connect motor and premotor areas. Conversely, activity during the uncrossed condition (LVF/LH) was confined to the right hemisphere in dorsal visual areas and motor-premotor cortices. This pattern replicates previous neuroimaging findings in healthy participants (17, 18, 23) and suggests that mechanisms of inter- and intrahemispheric transfer for normally perceived stimuli in G.Y. are comparable to those reported in neurotypical observers.

To reveal neural activity associated with nonconscious visuomotor processing we followed a two-step procedure. First, we compared brain responses to stimuli projected in the (blind) RVF vs. (intact) LVF (Fig. 2, *Middle* and Table S2). This contrast highlights only those areas that are differentially active when visual information is initially channeled to the V1-damaged hemisphere, irrespective of the hand used for the motor response. Bilateral activity was found in homologous areas of the dorsal stream, encompassing the banks of the intraparietal sulcus (IPS) and extending into the supramarginal gyrus (SMG), the precuneus (preCUN) principally in Brodmann Area (BA) 7M, and the isthmus of the CC. No functional response was detectable within the destroyed visual cortex. Activity for LVF stimuli was confined to the right striate and peristriate cortex. This indicates increased needs for interhemispheric communication between posterior dorsal areas specific for nonconscious visually guided action. Moreover, enhanced metabolic demands in the posterior segment of the CC suggest its pivotal involvement in this transfer of sensory-based information between corresponding regions of the two hemispheres.

Second, we performed the CUD comparison when responses were prompted by unseen RVF stimuli (Fig. 2, *Lower* and Table S3). This contrast bears evidence complementary to the previous one, as it discounts activity equally present in conditions of blind field stimulation to focus on neural mechanisms related to prepare and produce the manual response to unseen stimuli. Activation in the motor cortex was lateralized according to the hand used for responding. It is noteworthy that the uncrossed (RVF/RH) rather than the crossed condition (RVF/LH) yielded greater bilateral activity in areas corresponding to dorsal premotor (dPM), and supplementary motor cortex (SMA) (24) and in the anterior body of the CC. This is in agreement with RTs

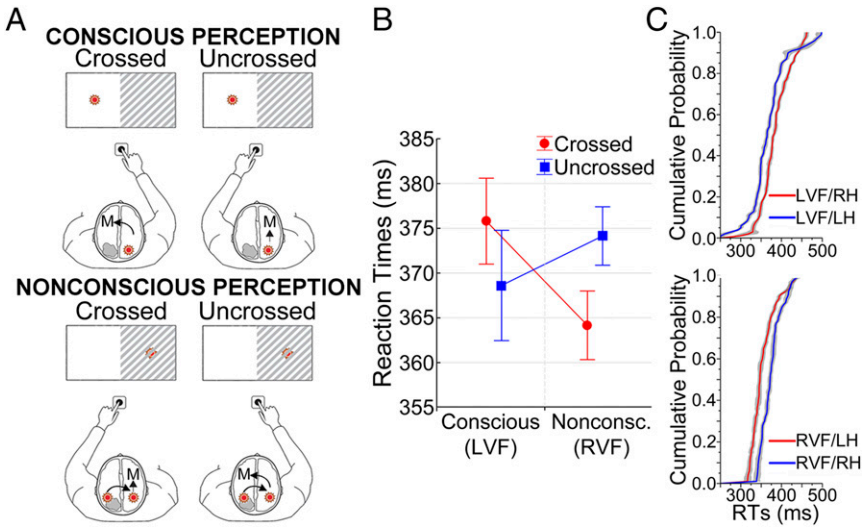

Fig. 1. Illustration of interhemispheric transfer and behavioral results. (*A*) Model proposed to interpret the CUD differences observed in RTs during conscious and nonconscious perception. (*B*) Mean RTs (± SEM) during conscious (LVF) and nonconscious (RVF) perception as a function of the crossed and uncrossed response conditions. (*C*) CDFs of RTs during conscious (*Upper Inset*) and nonconscious (*Lower Inset*) perception, as a function of the crossed (red lines) and uncrossed (blue lines) response conditions showing opposite patterns throughout the whole distributions.

data showing a negative CUD and indicates that access to premotor areas in the V1-damaged hemisphere of G.Y. requires additional interhemispheric transfer, rather than a simple relay from spared extrastriate areas to motor centers along the anteroposterior axis of the same (left) V1-lesioned hemisphere.

Pathways of Information Flow. Our hypothesis that simple visuomotor transformation in blindsight engages the intact hemisphere implies that (*i*) visual information entering extrastriate areas in the V1-lesioned hemisphere crosses to the intact hemisphere irrespective of the response hand (i.e., in both crossed and uncrossed conditions), (*ii*) this information is sent back from the (right) intact hemisphere to premotor centers of the (left) V1-damaged hemisphere only when a response with the RH is required (i.e., in the uncrossed RVF/RH condition), and (*iii*) activity in dorsal stream and premotor areas of the damaged hemisphere is unrelated

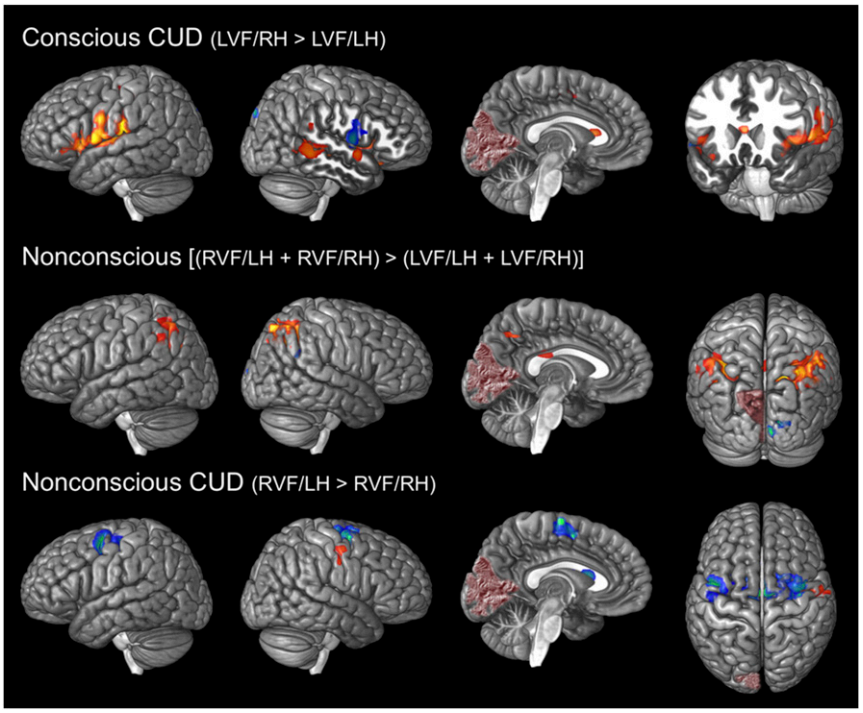

Fig. 2. Brain activity during conscious and nonconscious perception. The areas are significantly activated for each specified contrast at $P < 0.05$ corrected for FDR. Areas colored from red to yellow are significantly more active for crossed vs. uncrossed conditions during conscious perception (*Upper*), for nonconscious perception irrespective of response hand (*Middle*), and for the crossed vs. uncrossed conditions during nonconscious perception (*Lower*). The opposite holds for areas colored from blue to green. The lesion in the left V1 of G.Y. is visible and represented in dark red.

when the compensatory effects of the intact hemisphere are controlled for.

To examine information flow during blind RVF stimulation we analyzed trial-by-trial correlations in the signal intensity of brain activity between dorsal stream and premotor areas of the same and different hemispheres as a function of crossed and uncrossed response conditions (Fig. 3). Consistent with the notion that visual information transverses transcallosally between hemispheres, activity in the left and right IPS was correlated during crossed (RVF/LH) as well as uncrossed (RVF/RH) response conditions (crossed: Pearson $r = 0.41$, $P = 0.029$; uncrossed: $r = 0.43$, $P = 0.017$; all *Ps* are corrected with Hochberg's step-up procedure for familywise error rate). In contrast, activity in dPM/SMA areas of the (right) intact hemisphere was correlated with fMRI response in the corresponding regions of the (left) V1-lesioned hemisphere only during the uncrossed condition (crossed: $r = -0.07$, $P > 0.5$; uncrossed: $r = 0.42$, $P = 0.028$), a result that survived also when partialing out the effects of left and right dorsal stream areas ($r \geq 0.4$, $P \leq 0.031$). Finally, activity in visual and premotor areas within the V1-damaged hemisphere was uncorrelated in either response condition ($r \geq -0.15$, $P \geq 0.24$), whereas intrahemispheric responses in the right IPS and dPM/SMA areas of the intact hemisphere were significantly correlated, also when partialing out the effects of the V1-lesioned hemisphere (crossed: $r = -0.47$, $P = 0.006$; uncrossed: $r = 0.42$, $P = 0.048$).

These findings support our contention that the routing of visual information from the damaged to the intact hemisphere sustains nonconscious vision. Moreover, translating this visual input into motor output is contingent upon the functional compensation of the intact hemisphere and requires an additional interhemispheric cross-talk at the premotor level. This is indicated by significant trial-by-trial correlation between premotor areas of the two hemispheres only when the sensory signal and response hand are in the same contralesional (right) side.

fMRI-Guided Tractography. As was previously done to confirm and cross-validate functional activity detected in the CC (25), we have combined the complementary information of diffusion-weighted MRI (DW-MRI) and probabilistic tractography with fMRI to directly assess the relationship between structural and function brain properties. This enabled us to determine whether functional networks including gray and white matter activations under specific interhemispheric task demands colocalize with reconstructed fiber tracts connecting these areas. Fig. 4*A* displays the connectional fingerprint of functionally defined areas coactivated with callosal clusters, as determined by previous fMRI comparisons.

Three findings were observed in the normalized pattern of structural network configuration. First, reconstructed fibers transecting the rostral regions of the CC were predominantly connected with functionally responsive areas in the frontal lobe [t (34) = 4.67, $P < 0.0001$], whereas streamlines traversing the isthmus were linked with posterior parietal and temporal cortices [t (34) = 3.2, $P = 0.003$]. Second, connections between corresponding regions in opposite hemispheres (i.e., homotopic connections) were significantly prevalent over heterotopic connections or intrahemispheric tracts [F (2, 129) = 79.9, $P < 0.0001$]. Third, callosally mediated connections with cortical areas were bilateral and fairly symmetrical. Hence, functional covariance of fMRI signals in the CC and in cortical

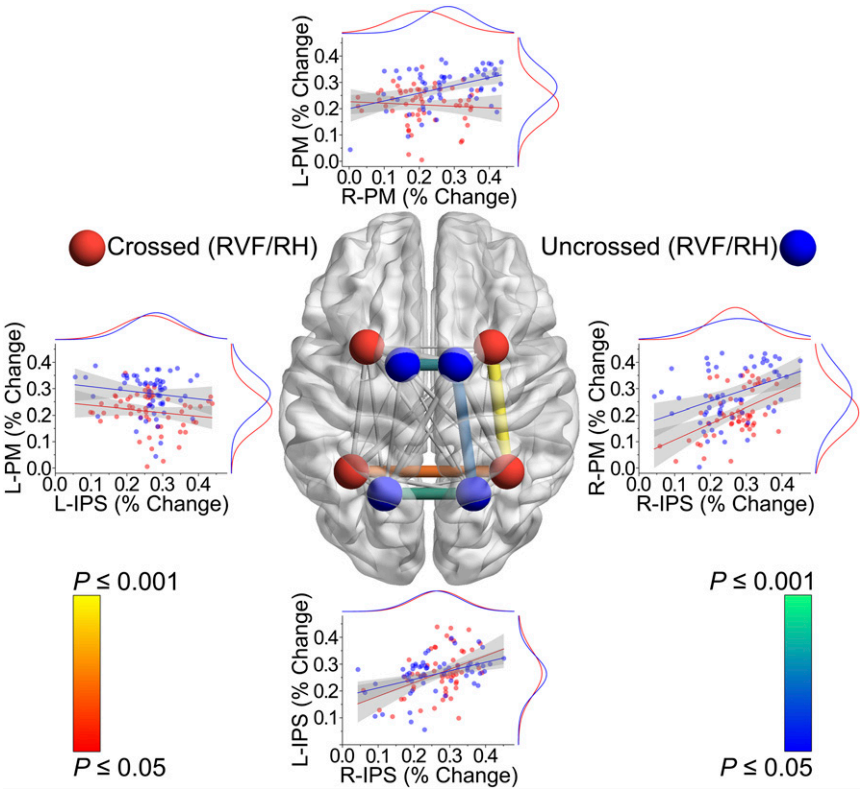

Fig. 3. Correlations in fMRI percent signal change during nonconscious perception. All possible correlations between left (L-) and right (R-) IPS and left and right premotor cortex (PM) as a function of crossed and uncrossed response conditions are displayed in the central transparent brain. The four areas are symbolized by spheres of different colors for the crossed (red) and uncrossed (blue) conditions. Edges diameter represents Pearson *r* value, whereas edges color represents *P* value. Nonsignificant correlations are shown in transparent gray. Lateral insets report scatterplots for the eight most relevant correlations. Marginal curves show the distribution of the data along *X* and *Y* axes, internal lines represent fitted correlations, and gray areas show 95% confidence limits.

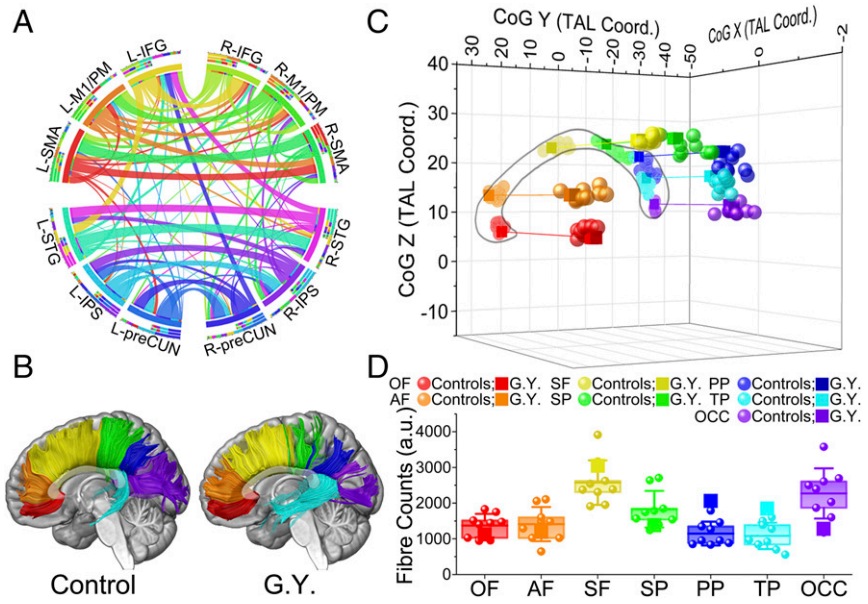

Fig. 4. Connectional, topographic, and microstructural properties of the CC. (*A*) Circular representation of the connectional fingerprint associated with cortical areas coactivated with the CC. Segments represent different areas and ribbons fiber tracts. Connections between areas in opposite hemispheres that did not course through the activated clusters in the CC are not displayed. (*B*) Tractographic segmentation of callosal fibers based on cortical projections in patient G.Y. and one representative control. Color codes for the seven callosal subregions are the same as those reported in the legends of *C* and *D*. (*C*) Three-dimensional representation of the CoG for each callosal compartment in the control subjects (circles) and G.Y. (squares). (*D*) Fiber counts for each callosal sector in the controls and G.Y. Box represents 25th and 75th percentiles, internal line represents controls mean, and whiskers represent SD. AF, anterior frontal; OCC, occipital; OF, orbitofrontal; PP, posterior parietal; SF, superior frontal; SP superior parietal; TP, temporal.

regions seems mediated by underlying anatomical projections. Furthermore, the segregation of these projections suggests a preserved topographic organization of callosal connections, as described below.

Topographic and Microstructural Changes in the CC. Due to the absence of macroscopic landmarks that delimit unambiguously distinct callosal compartments, several geometric subdivisions of the CC have been proposed (26, 27). However, these vertical segmentations do not always reflect functional partitions of the CC and are liable to its established morphological variability (28). Therefore, we have applied diffusion tensor imaging (DTI) to examine the topographic segmentation of the CC based on the separation of callosal fiber tracts with respect to their cortical projections (27, 29, 30).

We reconstructed seven callosal compartments according to their cortical projections, which distinguish fibers associated with orbitofrontal, anterior frontal, superior frontal, superior parietal, posterior parietal, temporal, and occipital regions. This arrangement of subdivisions was clearly discernible in the midsagittal cross-section of the CC and was highly coherent across G.Y. and age-matched controls (Fig. 4*B*). To quantify possible geometric differences in the topology of CC segmentation we computed the mean 3D center of gravity (CoG) for each of the seven callosal clusters in the control sample and then compared the distances with the corresponding CoGs in G.Y. (Fig. 4*C*). The topographic organization of the seven callosal segments was preserved in G.Y., as no significant spatial misalignment was observed with respect to controls [distance from mean CoGs $\leq$ 4.67 mm; t (8) $\leq$ 1.29, $P \geq 0.12$, all P values corrected with Crawford's procedure].

Finally, we investigated microstructural changes in the strength of transcallosal homotopic connections between G.Y. and controls for each subdivision of the CC (Fig. 4*D*). We found hypernormal callosal projections in G.Y. linking left and right posterior parietal cortices [t (8) = 2.59, $P = 0.03$], whereas differences from controls in the connections through other callosal sites did not survive to our conservative approach. Nevertheless, two additional trends consistent with previous tractography reports in G.Y. were observed (31, 32); namely, the connection strength between temporal areas was enhanced and approached significance [t (8) = 1.96, $P = 0.08$], whereas callosal fibers connecting the occipital lobes were reduced in number [t (8) = −1.34, $P = 0.21$].

Discussion

The present study examined the possible contribution of the intact hemisphere to the visual guidance of simple unimanual responses in blindsight, a condition typified by spared visuomotor abilities despite the loss of conscious vision following V1 damage (6, 7). Results support a dynamic model of interhemispheric plasticity and reorganization wherein sparing of functions can be attributed to the compensatory role of cortical areas in the undamaged hemisphere through transcallosal mediation. The concordance of cross-regional functional, structural, and connectional reorganization enabled us to delineate the features of neural reorganization that likely permit one to overcome the effects of early V1 lesion during the Poffenberger task. The most noteworthy findings are discussed below in separate sections.

Compensatory Role of the Intact Hemisphere. There are several theories on recovery of functions that similarly postulate substantial rebuilding in the aftermath of the lesion but emphasize different mechanisms, including compensation by perilesional cortex or homologous areas in the opposite hemisphere, subcortical structures, unmasking, or diaschisis reversal (1, 2, 33). At least two criteria have been established to consider differences in cortical activity as compensatory (34).

First, novel activity not observed in control conditions should arise specifically in response to demands placed to the damaged hemisphere. Consistent with this principle, when behaviorally relevant stimuli were presented in the blind RVF, thereby challenging the damaged visual system, dorsal stream areas in the IPS and BA 7M of the intact hemisphere selectively increased activity.

Recruitment of the contralesional dorsal stream cortex arguably originates from homologous regions of the affected hemisphere receiving V1-independent visual input from ipsilateral retino-recipient subcortical structures (e.g., inferior pulvinar) (11). This is evident from positive correlation of signal intensity between left and right parietal cortices during nonconscious visual processing and by concomitant enhancement of blood oxygen level-dependent (BOLD) response in the isthmus of the CC, where fibers connecting parietal regions converge.

Complementarily, the fact that activity over premotor cortex in the (right) intact hemisphere increased when the V1-damaged hemisphere had to control the RH response to ipsilateral stimuli (i.e., in the uncrossed RVF/RH condition) suggests that the intact hemisphere contributed dynamically to assist the V1-damaged hemisphere in premotor labor and visuomotor transformation. This surmise is further corroborated by evidence of (*i*) slower RTs in the uncrossed compared with crossed responses only for unseen RVF stimuli, (*ii*) associated covariance of activity between left and right premotor cortices, (*iii*) condition-specific increase of BOLD signal in the genu of the CC where premotor fibers course, and (*iv*) lack of significant correlation between parietal and prefrontal signal within the V1-damaged hemisphere.

Second, the putative compensatory activity must be associated with correct behavioral outcomes. G.Y. was clearly proficient in responding with either hand to visual stimuli projected to the affected visual hemifield, despite failing to acknowledge conscious perception. In fact, he missed responses to only 4/120 (3.3%) stimuli in his blind RVF, and RTs were almost identical to those recorded for normally seen stimuli when responses with the LH and RH were pooled together (Fig. 1*B*). These observations satisfy the second criterion and point to a subsidiary mechanism that can lead to adept performance levels by recruiting the intact hemisphere, at least in the elementary form of visuomotor functions tested here.

Altered Mechanisms of Callosal Interhemispheric Transfer. The behavioral, functional, and anatomical properties of interhemispheric transfer in the Poffenberger paradigm have been under scrutiny for decades (12, 14–18, 22, 23, 25) and involved assays of healthy participants as well as patients with agenesis or resection of the CC. Although results have not been always consistent, the bulk of the data suggests that the CUD reflects conduction delay across hemispheres (13), rather than the lowering of the activation threshold when visual stimulation primes the same hemisphere controlling manual response (35). Furthermore, it appears that visuomotor interhemispheric conduit occurs mainly at the premotor level, and the most likely route involves anterior sectors of the CC. Findings gathered in G.Y. during conscious visual perception agree with this picture.

To our knowledge, only one behavioral study has examined interhemispheric transfer of visuomotor information during nonconscious perception in blindsight patients (22). Faster responses were found in the crossed compared with the uncrossed condition, resulting in a negative CUD. Hence, the present study lends support to these prior findings and has implications for understanding the neurophysiological repercussions of V1 damage on interhemispheric integration, knowledge that could not be deduced from previous observations. Moreover, the fact that similar behavioral results were obtained in patients suffering brain damage in adulthood suggests that plastic mechanisms reported here in patient G.Y. might also occur in the mature brain.

At the cortical level we found enhanced activity in a bilateral network that primarily serves nonconscious visually guided action (9, 10, 36) and encompasses posterior parietal and frontal premotor areas. The posterior parietal cortex is endowed with premotor properties (37, 38), has extensive functional and anatomical connections with dPM cortices (36), and its damage lengthens interhemispheric transmission in the Poffenberger task (39). Furthermore, the ipsilesional extrastriate cortex seems uniquely positioned to pass visual information to homologous areas of the intact hemisphere at a relatively early stage, after stimulus onset. In fact, magnetoencephalography (MEG) in G.Y. has revealed that visual input relayed to the blind hemifield bypasses standard information flow along the cortical hierarchy, as activity is initially detected in contralateral higher-order visual areas as early as 100 ms after stimulus onset (40). Finally, activity in the precentral gyrus at sites compatible with the human location of dPM and SMA (24) is well known for its importance in response preparation as well as stimulus–response associations (41), and has been reported during simple voluntary movements triggered by visual stimuli (42).

Our findings suggest a notable role of the CC in synchronizing responses across homotopic regions of the posterior parietal and premotor cortices, thereby modulating the formation of neuronal assemblies across hemispheres (43, 44). By maintaining stable functional communication between hemispheres (45), the CC seems to afford an integral mechanism that adaptively compensates for V1 damage and sustains efficient visuomotor integration. This is confirmed by the fact that fMRI signal was detected in the genu and splenium of the CC during increased demands of interhemispheric transfer, and cooccurrence of functional activity in callosal and cortical regions was reflected in the presence of underlying projections crossing the CC. While geometrical and topological properties of the CC were not measurably altered in G.Y., we found an increased number of reconstructed fiber tracts connecting posterior parietal cortices and coursing through the splenium.

Evidence about restructuring of callosal connections following cortical damage in humans and animals is compelling (46). We speculate that the functional meaning of interhemispheric communication at posterior callosal sites is that of transferring sensory-based information. This would benefit from structural changes and rewiring contingent upon increased needs of compensatory visual processing following V1 damage. Conversely, callosal transmission at the anterior premotor level should mainly have modulatory rather than driving effects. These would consist of either transferring visuomotor information or assisting the V1-damaged hemisphere in the motor response. Because sustaining structural plasticity in long-range communication is costly in terms of energy consumption (47), as it entails sprouting, rebranching of fibers, or changes in other morphological features, enhanced interhemispheric communication at this premotor level may only take place upon task demands without underlying connectional modifications.

Relevance to Interpretation of Other Manifestations of Blindsight. Direct investigations on the contribution of the intact hemisphere to blindsight have been desultory, at least with respect to simple visuomotor functions. However, results compatible with a takeover of the undamaged hemisphere have been reported at different levels, and with a variety of methods.

Functionally, presentation of visual stimuli in the blind hemifield yields activity also in extrastriate cortices of the intact hemisphere, instead of triggering responses only in the contralateral hemisphere (48, 49). Anatomically, some blindsight patients have fiber tracts that connect subcortical visual structures in the V1-damaged hemisphere with cortical areas in the ipsilateral as well as contralateral hemisphere (31, 50), whereas only ipsilateral connections are normally found in healthy controls. Moreover, enhanced transcallosal connections between hMT/V5 areas have been reported in G.Y. (31). Behaviorally, these patients consciously experience flashes of light—phosphenes—in the blind hemifield uniquely when transcranial magnetic stimulation (TMS) is applied over both hemispheres simultaneously (51), whereas unilateral stimulation is sufficient to generate phosphenes in the contralateral visual hemifield of healthy subjects. Similarly, conscious experience of color induced by TMS-chromatic adaptation

seems to depend on stimulation of the intact hemisphere (52). Finally, hemianopic completions, which refer to perceptual completion of contours that straddle the vertical meridian into the blind hemifield (53), are associated with activity in the intact hemisphere (54).

Besides the CC and cortical structures reported here, other mesencephalic and diencephalic pathways exist to relay visual input to the contralateral side of the brain, and additional subcortical structures may serve as an interface between visual and motor processing. One obvious candidate is the superior colliculus, and the intercollicular commissure, that has been previously implicated in visuomotor blindsight (55) and whose stimulation can induce arm movements (56). Midline crossing may also occur downstream, as neurons in the pons receive visual input from dorsal stream cortices as well as from the superior colliculus and then project to the cerebellum, which in turn exerts control over descending motor tracts (57). Another possibility includes a pathway via the caudate nucleus, which receives projections from nearly all visual cortices, including IPS and BA 7, except from V1 (58). Knowledge about these alternative pathways derives chiefly from nonhuman studies. Therefore, their actual relevance for visuomotor functions in the V1-damaged human brain awaits further investigation.

Limitations. A number of limitations should be acknowledged and cautious remarks made accordingly.

First, our tentative interpretation about synchrony in interhemispheric assemblies, about the role of the CC in its generation, and about the unfolding of information flow in the sequence of brain events was based on cooccurrence of fMRI activity in GLM analysis and on trial-by-trial correlations of BOLD signal, respectively. This seems a reasonable hypothesis, considering that congruent visual stimuli synchronize activity between hemispheres, as shown with single-neuron recordings in cats, and that transection of the CC abolishes the effect (59). Moreover, similar results of increased interhemispheric coherence due to visual stimulation were reported with EEG recordings in humans (60), and increased coherence in EEG is linearly related to increase of BOLD signal in extrastriate areas (61). However, our interpretation remains speculative and also incorporates an element of directionality that needs more direct testing.

Second, we detected significant fMRI activations in the CC with BOLD contrasts, an issue that has gained considerable attention in recent years (62). There is evidence that the white matter has the vascular capacity to support hemodynamic changes detectable by fMRI (63), but the neurophysiological bases of activity-dependent hemodynamic changes are not fully resolved yet. BOLD signal change has been traditionally related to local field potentials, which do not take place in axons (64). However, a relationship between action potentials, which reflect the primary neuronal activity in white matter, and BOLD signal change has been reported more recently (65, 66). Moreover, activity-dependent metabolic changes in the CC have been established, as glucose consumption in the CC correlates with electrical stimulation of connected cortex (67). As a matter of fact, an increasing number of fMRI studies from different laboratories report activity in the CC, especially in relation to tasks like the Poffenberger paradigm that enhance interhemispheric communication through the CC (17, 18, 25, 62). In the present study we have tried to cross-validate activity in the CC in two ways. First, callosal activity varied as a function of specific task demands associated with increased needs for interhemispheric transmission, as shown in GLM comparisons between crossed and uncrossed conditions. Second, the relation between activity in the CC and cortex was assessed and linked to underlying structural connections. Admittedly, the issue of fMRI activity in the white matter requires further investigation, but we consider that the present findings cannot be simply dismissed as artifactual, and we adhere with the view that no direct evidence precludes the possibility of detecting fMRI activation in the CC (62).

Summary

The brain is naturally resilient to injury, and sparing or recovery of functions is generally attributed to reorganization in intact areas, a mechanism originally termed by Teuber (68) as the Kennard principle. The possibility to intervene in promoting recovery rests with our ability to understand the nature of postlesional plasticity and functional compensation (69). The main thrust of the present study is to have provided behavioral, functional, and connectional evidence about the compensatory role of the intact hemisphere and CC in residual visuomotor functions following early visual cortex damage. Hopefully, this can set a framework for future investigations on other adaptive mechanisms of compensation and functional recovery.

Methods

Subjects. Patient G.Y. suffered right hemianopia with macular sparing at the age of 8 y, following selective destruction of his left striate cortex as the result of traumatic brain injury (19). His blindsight abilities, as well as the functional and anatomical properties of his lesion, have been extensively characterized in previous behavioral (70), fMRI (21, 55), MEG (40), and tractography studies (31, 32). G.Y. was aged 56 at the time of testing.

Ten age- and gender-matched controls were scanned with a DW-MRI protocol and served as comparison for the assessment of topological and microstructural properties in the CC (mean age = 55.9 y; SD = 5.1). One participant was discarded because of movement artifacts. Informed consent was obtained from all participants.

Informed consent was obtained from patient G.Y. as well as from all healthy participants, and the study was approved by the Ethics Committee of the University of Turin, in accordance with the ethical standards laid down in the Declaration of Helsinki.

Stimuli and Procedure. A white square (90 cd/m^2) subtending 5° served as visual stimulus. It was presented for 200 ms against a dark background (20 cd/m^2) either in the LVF or RVF, with the innermost edge at 7° of eccentricity from a central fixation cross. To prompt attention and ensure central fixation, the cross changed color from black to red in a random interval varying from 200 ms to 1,700 ms before stimulus onset. Interstimulus interval was jitter from 2,100 ms to 12,100 ms. Stimulus presentation and response recording were controlled with Presentation software (NeuroBehavioral Systems).

G.Y. was asked to fixate the cross and press a response button positioned on the sagittal midplane of the trunk with his index finger as quickly as possible following stimulus detection. When the stimulus was projected in his blind RVF, he was required to "guess" stimulus onset. Eye movements were monitored with an MRI-compatible infrared camera connected to an eye-tracking system that analyzed online monocular pupil and corneal reflection (sampling rate 50 Hz). When inquired at the end of each block of trials, G.Y. never reported conscious perception of the stimuli in his blind RVF or light scatter from the blind to the intact field.

A mixed design was used, and four blocks of 60 trials each were administered, for a total of 240 trials. Stimuli were randomly presented in the LVF or RVF within each block, whereas response hand was alternated between blocks according to an ABBA design (A = LH and B = RH). G.Y. missed 8/240 (3.3%) trials overall, equally distributed between visual fields and response hands.

MRI Data Acquisition and Preprocessing. Data acquisition was performed on a 3-Tesla Siemens Magnetom Allegra scanner (Siemens). T2*-weighted fMRI images covering the whole brain were acquired using an EPI sequence (TR/TE/flip angle = 2,250 ms/25 ms/90°; field of view = 224 mm; acquisition matrix = 128 × 128; 42 contiguous 3.5- × 3.5- × 2.5-mm axial slices). Three-dimensional T1-weighted structural images were collected using a magnetization-prepared rapid gradient echo sequence (ADNI MPRAGE; TR/TE/flip angle = 2,250 ms/2.6 ms/ 9°; field of view = 256 mm; acquisition matrix = 256 × 256; 192 contiguous 1-mm^3 slices).

Preprocessing was performed with Brain-Voyager QX software (Brain Innovation) and included spatial realignment, slice scan time correction, 3D motion correction, and temporal filtering. The gray and white matter were segmented for each subject on T1-weighted anatomical images. G.Y.'s functional data were coregistered with his structural scan and normalized into Talairach space.

GLM Analysis of fMRI Data. Functional MRI data series were submitted to a single-subject analysis for event-related designs. The four experimental conditions (i.e., LVF/LH, LVF/RH, RVF/RH, and RVF/LH) were modeled by boxcar waveforms and convolved with the hemodynamic response function. Whole-brain analysis was performed, and a statistical threshold of $P < 0.05$ corrected for false discovery rate (FDR) in multiple comparisons was used. Cluster size threshold >20 contiguous voxels was applied. Activation maps were rendered with MRIcroGL on a standard 3D brain with the 3D reconstruction of G.Y.'s lesion superimposed.

Correlations of BOLD Signal Change. Four regions of interest (ROIs) were defined in the left and right IPS and PM cortex. These ROIs correspond to the clusters of voxels significantly activated in the GLM comparisons involving blind RVF stimulation (i.e., areas reported in Fig. 2, *Middle* and *Lower* and Tables S2 and S3). Voxels in dPM and SMA were pooled together because of spatial proximity. The maximum percent of BOLD signal change from baseline was extracted and then averaged across voxels within each ROI on a trial-by-trial basis and for crossed (RVF/LH) and uncrossed (RVF/RH) response conditions separately.

Pairwise Pearson's correlations were performed between signal changes in the 4 ROIs × 2 response conditions, resulting in a set of 28 *r* values with associated *Ps*. Hochberg's (71) step-up procedure was applied to correct for family-wise errors. It consists of a sequentially rejective procedure that contrasts the rank-ordered *P* values with a set of critical values and rejects all hypotheses with smaller or equal *Ps* to that of any one found less than its critical value. Briefly, *P* values are rank-ordered from smallest to highest, and correlations are deemed significant if $P_{(i)} \leq \alpha/m–i+1$, where *i* is the position of that *P* value in the rank order and *m* is the total number of the correlations performed. In the present case, the correlation associated with the smallest *P* value, thus ranking first in the list, is retained as significant if its $P \leq 0.00178$ [$P_{(1)} \leq 0.05/28 - 1 + 1$], the second if $P \leq 0.00185$, and so on.

DW-MRI Data Acquisition and Preprocessing. DW-MRI data were acquired in the same scanner at 2-mm^2 isotropic voxel resolution using spin echo echo-planar imaging and a standard head coil (TR/TE/flip angle/slice thickness/acquisition matrix = 8,600 ms/79 ms/90°/2 mm/128 × 104). Diffusion weighting was performed along 54 independent directions with a *b* value of 1,000 s/mm^2. A total of 75 slices covering the whole brain were acquired.

Diffusion data were preprocessed with FMRIB Diffusion Toolbox implementing standard eddy current and motion correction pipelines (72). DW-MRI images of G.Y. and nine controls were coregistered with the respective structural scans using boundary based registration and normalized into Talairach space.

fMRI-Guided Tractography. Brain areas functionally responsive in the different GLM contrasts on fMRI data were transformed into diffusion space and served as ROIs for probabilistic fiber tracking, which was performed with Bedpostx and Probtrackx2 scripts in FSL (73). Probabilistic tractography is estimated from two possible fiber orientations for each voxel and infers the most likely trajectories of reconstructed streamlines between ROIs, thus enabling modeling of crossing fibers in the voxels (probtrackx2: 5,000 samples, curvature threshold = 0.2, modified Euler integration).

Reconstructed tracts were categorized into interhemispheric pathways coursing through the anterior or posterior ROIs in the CC and intrahemispheric pathways connecting ipsilateral cortical ROIs without involving the CC. Based on visual inspection of the trajectories, interhemispheric tracts crossing the anterior and posterior CC ROIs were further categorized into those connecting homotopic and heterotopic regions. Independent sample *t* tests and one-way ANOVA on normalized fiber counts for each bundle were used to test for significant difference in the nature and spatial distribution of the tracts.

Assessment of Topographic and Connectional Properties of the CC. Tractography-based segmentation of the CC applied a modified version of the procedure described by Huang et al. (29) and Hofer and Frahm (27). A first reference ROI was drawn on the midsagittal plane to include the entire CC. The second set of ROIs was placed close to the cortex according to anatomical landmarks and separated transcallosal projections targeting the orbitofrontal, anterior frontal, superior frontal, superior parietal, posterior parietal, temporal, and occipital regions, along the anterior–posterior axis. Each callosal ROI was defined independently in G.Y. and the nine controls, and each pericortical ROI was further defined independently for the left and right hemisphere.

Deterministic fiber tracking performed with ExploreDTI assigned each voxel in the CC to fibers belonging to one of the seven cortical areas [fractional anisotropy (FA) threshold = 0.2; angle threshold = 35°]. This resulted in the natural and data-driven segmentation of the CC in seven vertical subdivisions based on the outcome of streamline tractography. Streamlines count and FA values were calculated for each callosal compartment and participant independently. Voxels in CC containing tracts from two or more segments were not assigned to any callosal compartment and removed from analysis, as well as voxels not crossed by fibers from/to pericortical ROIs.

The CoG was computed for every callosal subregion and for each participant independently, as the weighted average of the *X*, *Y*, and *Z* coordinates by the intensities within each CC cluster. We then calculated for patient G.Y. and every participant the 3D Euclidean distance from the mean CoGs in the control sample using the formula

$$EuD_{(p_i,q)} = \sqrt{\left(p_{i(X)} - q_{(X)}\right)^2 + \left(p_{i(Y)} - q_{(Y)}\right)^2 + \left(p_{i(Z)} - q_Z\right)^2},$$

where $p_{i(X,\,Y,\,X)}$ is the CoG of participant *i* in *X*, *Y*, and *Z* coordinates and $q_{(X,\,Y,\,X)}$ is the mean CoG in the control sample.

Statistically significant differences between the CoG of each callosal subregion in G.Y. and the CoGs in the corresponding subregions of the controls were assessed by a series of single-sample *t* tests. The method proposed by Crawford and Howell (74) has been applied to the *t* test results to correct for possible deviations from normality in relatively small samples of controls by considering control sample mean values as statistics rather than as parameters.

The same procedure and *t* tests were used to compare the density of callosal fibers tracts between G.Y. and controls for each subdivision of CC, as defined by the number of streamlines crossing that specific compartment.

ACKNOWLEDGMENTS. M.T. thanks Cristiano W. Di Tizio for helpful discussions on important aspects related to this manuscript and Dick Passingham for insightfully pointing out that activity in preCUN was compatible with the location of BA 7M. This work was supported by Netherlands Organization for Scientific Research Vidi Grant 452-11-015 (to A.C., M.D., and M.T.), Futuro in Ricerca 2012 Grant RBFR12F0BD, PRIN 2015 Grant 2015NA4S55 from the Italian Ministry of Education University and Research, a European Research Council (ERC) Advanced Grant under the European Union 7th Framework Programme (to B.d.G.), and an ERC Advanced Grant "Perceptual Awareness" under the European Union 7th Framework Programme (to C.A.M.).

1. Payne BR, Lomber SG (2001) Reconstructing functional systems after lesions of cerebral cortex. *Nat Rev Neurosci* 2:911–919.
2. Voytek B, et al. (2010) Dynamic neuroplasticity after human prefrontal cortex damage. *Neuron* 68:401–408.
3. Johansen-Berg H, et al. (2002) The role of ipsilateral premotor cortex in hand movement after stroke. *Proc Natl Acad Sci USA* 99:14518–14523.
4. Takatsuru Y, et al. (2009) Neuronal circuit remodeling in the contralateral cortical hemisphere during functional recovery from cerebral infarction. *J Neurosci* 29: 10081–10086.
5. Edelman GM, Gally JA (2001) Degeneracy and complexity in biological systems. *Proc Natl Acad Sci USA* 98:13763–13768.
6. Weiskrantz L (2009) *Blindsight: A Case Study Spanning 35 Years and New Developments* (Oxford Univ Press, Oxford), p 255.
7. Weiskrantz L, Warrington EK, Sanders MD, Marshall J (1974) Visual capacity in the hemianopic field following a restricted occipital ablation. *Brain* 97:709–728.
8. Rafal R, Smith J, Krantz J, Cohen A, Brennan C (1990) Extrageniculate vision in hemianopic humans: Saccade inhibition by signals in the blind field. *Science* 250: 118–121.
9. Goodale MA (2011) Transforming vision into action. *Vision Res* 51:1567–1587.
10. Milner AD, Goodale MA (2006) *The Visual Brain in Action* (Oxford Univ Press, Oxford).
11. Tamietto M, Morrone MC (2016) Visual plasticity: Blindsight bridges anatomy and function in the visual system. *Curr Biol* 26:R70–R73.
12. Poffenberger AT (1912) Reaction time to retinal stimulation with special reference to the time lost in conduction through nervous centers. *Arch Psychol* 23:1–73.
13. Berlucchi G, Heron W, Hyman R, Rizzolatti G, Umiltà C (1971) Simple reaction times of ipsilateral and contralateral hand to lateralized visual stimuli. *Brain* 94:419–430.
14. Marzi CA, Bisiacchi P, Nicoletti R (1991) Is interhemispheric transfer of visuomotor information asymmetric? Evidence from a meta-analysis. *Neuropsychologia* 29: 1163–1177.
15. Berlucchi G, Aglioti S, Marzi CA, Tassinari G (1995) Corpus callosum and simple visuomotor integration. *Neuropsychologia* 33:923–936.
16. Iacoboni M, Zaidel E (1995) Channels of the corpus callosum. Evidence from simple reaction times to lateralized flashes in the normal and the split brain. *Brain* 118: 779–788.
17. Weber B, et al. (2005) Attention and interhemispheric transfer: A behavioral and fMRI study. *J Cogn Neurosci* 17:113–123.
18. Tettamanti M, et al. (2002) Interhemispheric transmission of visuomotor information in humans: fMRI evidence. *J Neurophysiol* 88:1051–1058.

19. Barbur JL, Harlow AJ, Weiskrantz L (1994) Spatial and temporal response properties of residual vision in a case of hemianopia. *Philos Trans R Soc Lond B Biol Sci* 343: 157–166.
20. Tamietto M, et al. (2009) Unseen facial and bodily expressions trigger fast emotional reactions. *Proc Natl Acad Sci USA* 106:17661–17666.
21. Baseler HA, Morland AB, Wandell BA (1999) Topographic organization of human visual areas in the absence of input from primary cortex. *J Neurosci* 19:2619–2627.
22. Celeghin A, et al. (2015) Speeded manual responses to unseen visual stimuli in hemianopic patients: What kind of blindsight? *Conscious Cogn* 32:6–14.
23. Iacoboni M, Zaidel E (2004) Interhemispheric visuo-motor integration in humans: The role of the superior parietal cortex. *Neuropsychologia* 42:419–425.
24. Mayka MA, Corcos DM, Leurgans SE, Vaillancourt DE (2006) Three-dimensional locations and boundaries of motor and premotor cortices as defined by functional brain imaging: A meta-analysis. *Neuroimage* 31:1453–1474.
25. Mazerolle EL, et al. (2010) Confirming white matter fMRI activation in the corpus callosum: Co-localization with DTI tractography. *Neuroimage* 50:616–621.
26. Witelson SF (1989) Hand and sex differences in the isthmus and genu of the human corpus callosum. A postmortem morphological study. *Brain* 112:799–835.
27. Hofer S, Frahm J (2006) Topography of the human corpus callosum revisited–Comprehensive fiber tractography using diffusion tensor magnetic resonance imaging. *Neuroimage* 32:989–994.
28. Doron KW, Gazzaniga MS (2008) Neuroimaging techniques offer new perspectives on callosal transfer and interhemispheric communication. *Cortex* 44:1023–1029.
29. Huang H, et al. (2005) DTI tractography based parcellation of white matter: Application to the mid-sagittal morphology of corpus callosum. *Neuroimage* 26:195–205.
30. Lebel C, Caverhill-Godkewitsch S, Beaulieu C (2010) Age-related regional variations of the corpus callosum identified by diffusion tensor tractography. *Neuroimage* 52: 20–31.
31. Bridge H, Thomas O, Jbabdi S, Cowey A (2008) Changes in connectivity after visual cortical brain damage underlie altered visual function. *Brain* 131:1433–1444.
32. Tamietto M, Pullens P, de Gelder B, Weiskrantz L, Goebel R (2012) Subcortical connections to human amygdala and changes following destruction of the visual cortex. *Curr Biol* 22:1449–1455.
33. Merabet LB, Pascual-Leone A (2010) Neural reorganization following sensory loss: The opportunity of change. *Nat Rev Neurosci* 11:44–52.
34. Davis SW, Dennis NA, Daselaar SM, Fleck MS, Cabeza R (2008) Que PASA? The posterior-anterior shift in aging. *Cereb Cortex* 18:1201–1209.
35. Kinsbourne M (2003) The corpus callosum equilibrates the cerebral hemispheres. *The Parallel Brain: The Cognitive Neuroscience of the Corpus Callosum*, eds Zaidel E, Iacoboni M (MIT Press, Cambridge, MA), pp 271–281.
36. Kravitz DJ, Saleem KS, Baker CI, Mishkin M (2011) A new neural framework for visuospatial processing. *Nat Rev Neurosci* 12:217–230.
37. Fogassi L, et al. (2005) Parietal lobe: From action organization to intention understanding. *Science* 308:662–667.
38. Rizzolatti G, Matelli M (2003) Two different streams form the dorsal visual system: Anatomy and functions. *Exp Brain Res* 153:146–157.
39. Marzi CA, Bongiovanni LG, Miniussi C, Smania N (2003) Effects of partial callosal and unilateral cortical lesions on interhemispheric transfer. *The Parallel Brain: The Cognitive Neuroscience of the Corpus Callosum*, eds Zaidel E, Iacoboni M (MIT Press, Cambridge, MA), pp 287–295.
40. Ioannides AA, et al. (2012) Spatiotemporal profiles of visual processing with and without primary visual cortex. *Neuroimage* 63:1464–1477.
41. Passingham RE (1993) *The Frontal Lobes and Voluntary Action* (Oxford Univ Press, Oxford).
42. Picard N, Strick PL (2003) Activation of the supplementary motor area (SMA) during performance of visually guided movements. *Cereb Cortex* 13:977–986.
43. Innocenti GM (2009) Dynamic interactions between the cerebral hemispheres. *Exp Brain Res* 192:417–423.
44. Schmidt KE, Lomber SG, Innocenti GM (2010) Specificity of neuronal responses in primary visual cortex is modulated by interhemispheric corticocortical input. *Cereb Cortex* 20:2776–2786.
45. Shen K, et al. (2015) Stable long-range interhemispheric coordination is supported by direct anatomical projections. *Proc Natl Acad Sci USA* 112:6473–6478.
46. Restani L, Caleo M (2016) Reorganization of visual callosal connections following alterations of retinal input and brain damage. *Front Syst Neurosci* 10:86.
47. Bullmore E, Sporns O (2012) The economy of brain network organization. *Nat Rev Neurosci* 13:336–349.
48. Bittar RG, Ptito M, Faubert J, Dumoulin SO, Ptito A (1999) Activation of the remaining hemisphere following stimulation of the blind hemifield in hemispherectomized subjects. *Neuroimage* 10:339–346.
49. Goebel R, Muckli L, Zanella FE, Singer W, Stoerig P (2001) Sustained extrastriate cortical activation without visual awareness revealed by fMRI studies of hemianopic patients. *Vision Res* 41:1459–1474.
50. Leh SE, Johansen-Berg H, Ptito A (2006) Unconscious vision: New insights into the neuronal correlate of blindsight using diffusion tractography. *Brain* 129:1822–1832.
51. Silvanto J, Cowey A, Lavie N, Walsh V (2007) Making the blindsighted see. *Neuropsychologia* 45:3346–3350.
52. Silvanto J, Cowey A, Walsh V (2008) Inducing conscious perception of colour in blindsight. *Curr Biol* 18:R950–R951.
53. Torjussen T (1978) Visual processing in cortically blind hemifields. *Neuropsychologia* 16:15–21.
54. Weil RS, Plant GT, James-Galton M, Rees G (2009) Neural correlates of hemianopic completion across the vertical meridian. *Neuropsychologia* 47:457–464.
55. Tamietto M, et al. (2010) Collicular vision guides nonconscious behavior. *J Cogn Neurosci* 22:888–902.
56. Philipp R, Hoffmann K-P (2014) Arm movements induced by electrical microstimulation in the superior colliculus of the macaque monkey. *J Neurosci* 34: 3350–3363.
57. Glickstein M (2000) How are visual areas of the brain connected to motor areas for the sensory guidance of movement? *Trends Neurosci* 23:613–617.
58. Saint-Cyr JA, Ungerleider LG, Desimone R (1990) Organization of visual cortical inputs to the striatum and subsequent outputs to the pallido-nigral complex in the monkey. *J Comp Neurol* 298:129–156.
59. Engel AK, König P, Kreiter AK, Singer W (1991) Interhemispheric synchronization of oscillatory neuronal responses in cat visual cortex. *Science* 252:1177–1179.
60. Knyazeva MG, et al. (1999) Visual stimulus-dependent changes in interhemispheric EEG coherence in humans. *J Neurophysiol* 82:3095–3107.
61. Knyazeva MG, Fornari E, Meuli R, Innocenti G, Maeder P (2006) Imaging of a synchronous neuronal assembly in the human visual brain. *Neuroimage* 29:593–604.
62. Gawryluk JR, Mazerolle EL, D'Arcy RCN (2014) Does functional MRI detect activation in white matter? A review of emerging evidence, issues, and future directions. *Front Neurosci* 8:239.
63. Gardener AG, Jezzard P (2015) Investigating white matter perfusion using optimal sampling strategy arterial spin labeling at 7 Tesla. *Magn Reson Med* 73:2243–2248.
64. Logothetis NK, Pauls J, Augath M, Trinath T, Oeltermann A (2001) Neurophysiological investigation of the basis of the fMRI signal. *Nature* 412:150–157.
65. Nir Y, et al. (2008) Interhemispheric correlations of slow spontaneous neuronal fluctuations revealed in human sensory cortex. *Nat Neurosci* 11:1100–1108.
66. Smith AJ, et al. (2002) Cerebral energetics and spiking frequency: The neurophysiological basis of fMRI. *Proc Natl Acad Sci USA* 99:10765–10770.
67. Weber B, Fouad K, Burger C, Buck A (2002) White matter glucose metabolism during intracortical electrostimulation: A quantitative [(18)F]Fluorodeoxyglucose autoradiography study in the rat. *Neuroimage* 16:993–998.
68. Teuber HL (1974) Functional recovery after lesions of the nervous system. II. Recovery of function after lesions of the central nervous system: History and prospects. *Neurosci Res Program Bull* 12:197–211.
69. Ro T, Rafal R (2006) Visual restoration in cortical blindness: Insights from natural and TMS-induced blindsight. *Neuropsychol Rehabil* 16:377–396.
70. Weiskrantz L, Barbur JL, Sahraie A (1995) Parameters affecting conscious versus unconscious visual discrimination with damage to the visual cortex (V1). *Proc Natl Acad Sci USA* 92:6122–6126.
71. Hochberg Y (1988) A sharper Bonferroni procedure for multiple tests of significance. *Biometrika* 75:800–802.
72. Jenkinson M, Beckmann CF, Behrens TE, Woolrich MW, Smith SM (2012) FSL. *Neuroimage* 62:782–790.
73. Behrens TE, Berg HJ, Jbabdi S, Rushworth MF, Woolrich MW (2007) Probabilistic diffusion tractography with multiple fibre orientations: What can we gain? *Neuroimage* 34:144–155.
74. Crawford JR, Howell DC (1998) Comparing an individual's test score against norms derived from small samples. *Clin Neuropsychol* 12:482–486.